

Structural, magnetic properties and microwave absorbing behavior of iron based carbon nanocomposites

Mashadi, Yunasfi and Wisnu Ari Adi*

Centre for Science and Technology of Advanced Materials – National Nuclear Energy Agency, Kawasan Puspiptek Serpong, Tangerang Selatan, Banten, Indonesia15314.

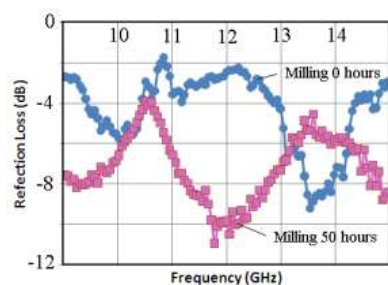
*Corresponding Author: mashadi@batan.go.id, mashadi71@gmail.com

Article history :

Received 31 December 2015

Accepted 14 January 2016

GRAPHICAL ABSTRACT



ABSTRACT

Nanocomposite of α -Fe/C was successfully synthesized by mechanical milling method Graphite powders with purity of greater than 99% were mixed with analytical grade of α -Fe. The mixture was milled for 50hours at room temperature using High Energy Milling (HEM). The refinement results of X-ray diffraction pattern shows that the α -Fe/C nanocomposite consists of 20 wt% Fe and 80 wt% C. The mechanical milling resulted in α -Fe/C powders with mean particle size \sim 900 nm. The image reveals the morphology of particle and the particles that exist is aggregates of fine grains. The magnetic properties of the particle α -Fe/C nanocomposite showed low coercivity and high remanent magnetization. The α -Fe/C nanocomposite has certain microwave absorber properties in the frequency range of 9 – 15 GHz, with the maximum reflection loss reaches -10 dB at 12 GHz and the absorption range under -4 dB is from 11.2 to 15.5 GHz with 2 mm thickness. The study concluded that the α -Fe/C nanocomposite shows good candidate materials for microwave absorbing materials applications.

Keywords: nanocomposite, α -Fe/C, magnetic, absorber, microwave.

© 2014 Penerbit UTM Press. All rights reserved
<http://dx.doi.org/10.11113/mjfas.v12n1.365>

1. INTRODUCTION

Electronic devices technology that work at high frequencies such as mobile phones, intelligent transportation systems, local area network systems, and radar systems have been growing rapidly. However, these electronic devices are usually impaired due to the presence of electromagnetic wave interference (EMI) [1]. One of way is needed a materials that can absorb electromagnetic waves that can effectively eliminate the EMI. Recently, among the candidates of EM absorbing materials, anti-EMI (electromagnetic interference) have attracted much attention as a soft metallic magnet [1-2] due to large saturation magnetization values and high frequency level of their Snoek's limit [3]. Consequently, these material will have high relative complex permeability (μ_r), indicating the possibility as thin absorbers. The complex permeability and permittivity of the materials determine the reflection loss and attenuation characteristics of the electromagnetic wave absorbers. However, the problem is that these materials have a high electrical conductivity, so that their permeabilities at high frequencies will decrease due to Eddy current loss caused by the electromagnetic wave [4]. To suppress Eddy current losses, it will require skin-depth for each particle. This means that the metallic soft magnetic

materials can be used as an electromagnetic wave absorber materials, the effective size of the nanoparticles were isolated by a non-conductive material of rare earth metal oxides.

In previous studies, Sugimoto *et.al* has managed to make composite α -Fe/SmO which has good EM absorption in the frequency range of 0.73 to 1.30 GHz. SmO nanoparticles act as an insulator embedded either or in the α -Fe particles to reduce Eddy current losses [4]. Likewise, Liu *et.al* has reported that the synthesized nanocomposites with structure of α -Fe/Y₂O₃, α -Fe/Fe₃B/Y₂O₃, ϵ -Fe₃N/Y₂O₃ have good absorption properties of electromagnetic in a different frequency range [5]. Although the study showed good absorption properties, the preparation process is relatively complicated and expensive because it uses rare earth metals. For this reason, it is necessary to develop new composites and the design process is relatively simple as electromagnetic absorption material.

According to Zhu *et.al*, they have reliably and economically prepared Fe-filled carbon nanotubes by pyrolysis of ferrocene and activated carbon [6]. Investigation of electromagnetic property and microwave absorbing behavior indicates that the as synthesized Fe-filled CNTs have potential applications in the fields of microwave absorbing materials. Therefore, we report the

successful preparation of nanocomposite graphite powder containing of α -Fe (α -Fe/C) with mechanical milling technique. In particular, we propose that the carbon structure in graphite powder can be used to replace the rare earth metal oxide as a separator between α -Fe particles in the hope of pressing the Eddy current losses. By investigating the EM wave absorption properties, it is expected that the resulting nanocomposites have potential applications in the fields of microwave absorbing materials.

2. EXPERIMENTS

The materials used in this study were the powder graphite (carbon, C) from Merck products (purity of 99.5% and particle size of 1–2 μ m) and iron powder (Fe) from Aldrich product (purity of 99.9% and various particle size of 2–10 μ m). Nanocomposite Fe-C powders are made from a mixture of Fe and graphite powders with a weight ratio of 1 : 4, respectively. The Fe and graphite powders were weighed in 10 g and then the mixture was transferred to a stainless steel type of 50 mL container/vial containing of balls. The weight ratio between ball and the sample were 3 : 2. The mixture was milled for 50 hours at room temperature using High Energy Milling (HEM) from SPEX8000M Mixer/Mill brand CertiPrep. This method is then called mechano-thermal.

The phase analysis of the sample was carried out by powder X-ray diffraction (XRD) using Miniflex Rigaku diffractometer with CuK- α radiation ($\lambda= 1.5406 \text{ \AA}$). The Rietveld analysis was performed on applying GSAS program [7]. The particle morphology of the sample was observed by using scanning electron microscope (SEM) and transmission electron microscope (TEM). The magnetic properties were measured by using vibrating sample magnetometer (VSM) with external magnetic field of about 1 Tesla at room temperature. Finally, the reflection and transmission of microwave were carried out using the vector network analyzer (VNA) with frequency range of 10 – 15 GHz.

3. RESULTS AND DISCUSSION

The identification results of XRD profiles on the α -Fe/C samples are shown in Figure 1. The XRD profiles have been compared between α -Fe/C before (Fe-C_mill-0h), after milling for 50 hours (Fe-C_mill-50h) and MWNT (multi-wall nano-tube), respectively.

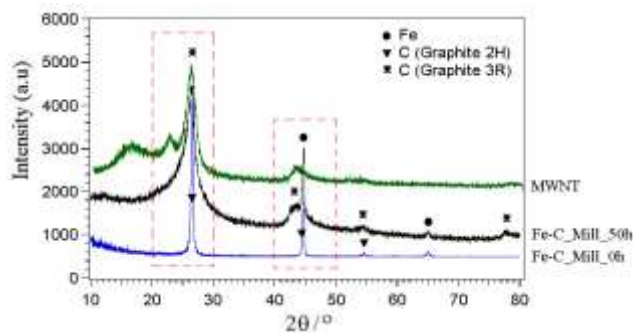


Fig. 1 XRD profile of all samples

Figure 1 show that the peak intensity of graphite looked down very significantly from 4800 a.u. down to 3700 a.u. after milled for 50 h. The milling process can cause the interlayer distance of graphite increases and amorphous process occurs well. During the milling process occur plastic deformation and fracture of particles, causing the particle size continuously reduced. The mechano-thermal has been known to be an effective way to prepare nanocrystalline structures and thus used to produce high surface area graphite.

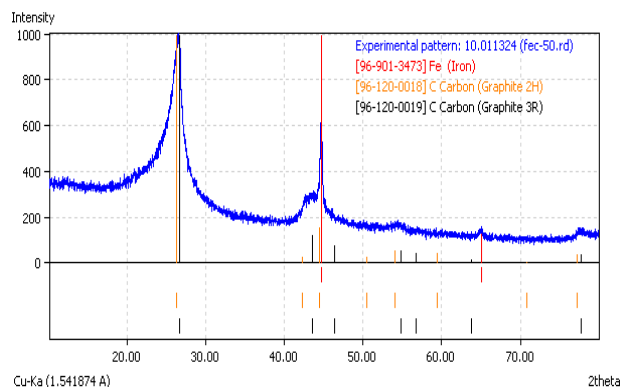
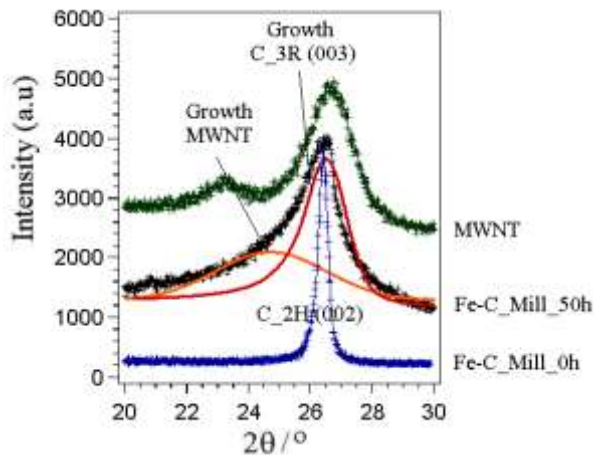
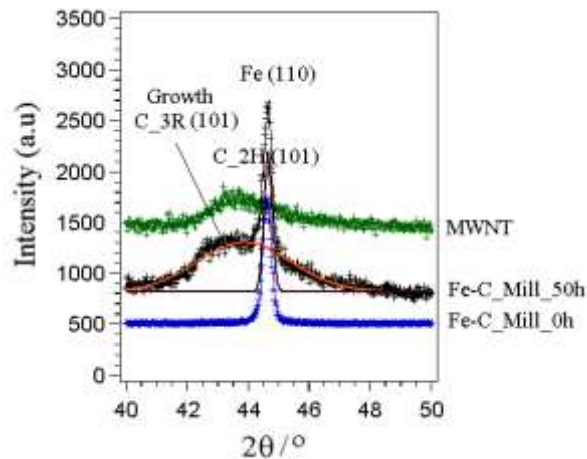


Fig. 2 Identification of XRD profile

Accordance to the Hanawalt table as shown Figure 2, the phase identification result shows that the graphite sample after milling for 50 hours consist of three phases, namely carbon (C_2H), carbon (C_3R) and iron (Fe) phases that respective referred to the research results of Fayos (COD-AMCSD-96-901-2231) [8], Lipson (COD-AMCSD-96-120-0019) [9] and Fjellvag (COD-AMCSD-96-900-2673) [10]. Hence, the resulting graphite composite through this method was transformed the phase of powder graphite from hexagonal carbon (C_2H) become to rhombohedral carbon (C_3R) structures as shown Figure 3(a).



(a) Diffraction profile of Fe-C_Mill_50h was compared by diffraction profile of MWNT at range 20°-30°



(b) Diffraction profile of Fe-C_Mill_50h was compared by diffraction profile of MWNT at range 40°-50°

Figure 3. XRD profile of graphite samples and MWNT

From Figure 3 (a), broadening of the C_{2H} (002) peak shows that the interlayer distance of graphite increased after milling process. The hexagonal carbon (C_{2H}) phase gradually transforms to a mixture of the amorphous phase and nano-crystallites through turbostatic structure. Graphite layers were partially broken due to both much reduced plastic deformation and agglomeration of particles during the mechano-thermal process. During milling process, this amorphous phase was crystallized by heat due to effect impact of milling process. That also shows that further changes even after treatment of the milled powders were observed to form nuclei of MWNT

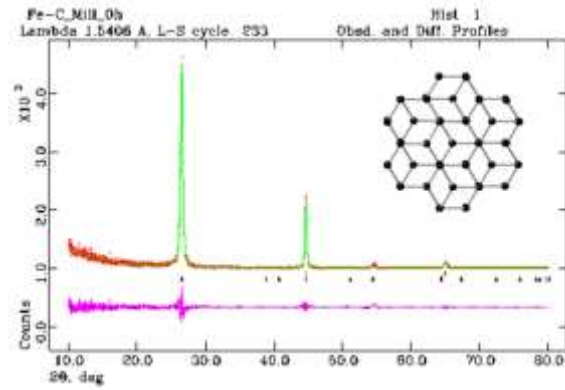


Fig. 4 Diffraction profile refinement of Fe-C_Mill_0h

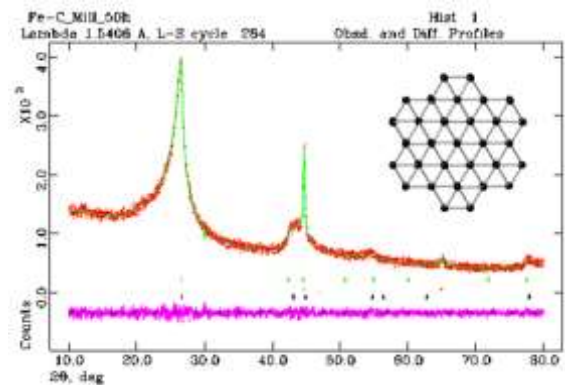


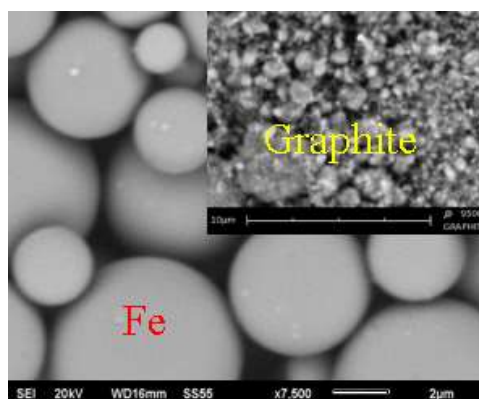
Fig. 5 Diffraction profile refinement of Fe-C_Mill_50h

The analysis of phase composition on the samples was analyzed by using the GSAS software as shown in Figure 4 and Figure 5. The quality factors of fitting on R (criteria of fit) and χ^2 (goodness of fit) have been valued as the minimum, and the allowed of χ^2 is less than 1.3 [11]. It means that the profile is in good agreement among the observation and calculations. The refinement results of x-ray diffraction pattern shows that the sample with milling time for 50 hours consist of three phases, namely carbon (C_{2H}), carbon (C_{3R}) and iron (Fe) phases with structure parameter, mass fraction, factor R and *goodness of fit* (χ^2) as shown in Table 1.

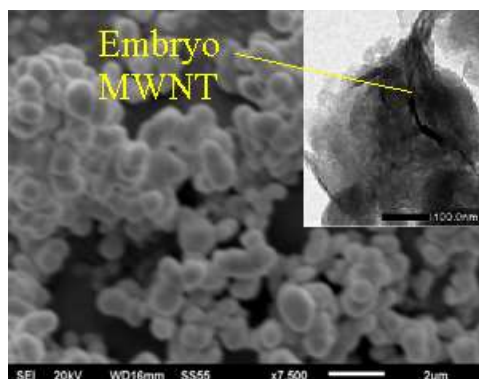
Table 1 Structure parameter, mass fraction, R factor and goodness of fit (χ^2)

α -Fe/C_mill-0h	α -Fe/C_mill-50h
• Carbon (C_2H) phase	• Carbon (C_2H) phase
Space group : P 63 m c (186), Hexagonal	Space group : P 63 m c (186), Hexagonal
$a = b = 2.449(6) \text{ \AA}$ and $c = 6.774(1) \text{ \AA}$, $\alpha = \beta = 90^\circ$ and $\gamma = 120^\circ$	$a = b = 2.563(2) \text{ \AA}$ and $c = 6.352(1) \text{ \AA}$, $\alpha = \beta = 90^\circ$ and $\gamma = 120^\circ$
$V = 62.5(2) \text{ \AA}^3$ and $\rho = 2.544 \text{ gr.cm}^{-3}$	$V = 41.8(1) \text{ \AA}^3$ and $\rho = 2.682 \text{ gr.cm}^{-3}$
Mass fraction = 79.79 wt%	Mass fraction = 62.83 wt%
Crystallite size = 494 nm	Crystallite size = 10 nm
• Iron (Fe) phase	• Iron (Fe) phase
Space group : F m -3 m (225), Cubic	Space group : F m -3 m (225), Cubic
$a = b = c = 2.871(1) \text{ \AA}$, $\alpha = \beta = \gamma = 90^\circ$	$a = b = c = 2.870(1) \text{ \AA}$, $\alpha = \beta = \gamma = 90^\circ$
$V = 23.67(2) \text{ \AA}^3$ and $\rho = 7.834 \text{ gr.cm}^{-3}$	$V = 23.64(3) \text{ \AA}^3$ and $\rho = 7.843 \text{ gr.cm}^{-3}$
Mass fraction = 20.21 wt%	Mass fraction = 20.23 wt%
Crystallite size = 672 nm	Crystallite size = 219 nm
• Carbon (C_3R) phase	• Carbon (C_3R) phase
Not found	Space group : R -3 m (166), Rhombohedral
	$a = b = c = 3.464(1) \text{ \AA}$, $\alpha = \beta = \gamma = 39.55(1)^\circ$
	$V = 35.16(7) \text{ \AA}^3$ and $\rho = 4.522 \text{ gr.cm}^{-3}$
	Mass fraction = 16.94 wt%
	Crystallite size = 8 nm
wRp = 1.93 and χ^2 (chi-squared) = 1.040	wRp = 4.69 and χ^2 (chi-squared) = 1.208

Accordance to the refinement result of XRD profile, it is shown that the composition of the composite samples still suitable with composite composition (Fe and graphite powders with a weight ratio of 1 : 4, respectively). Figure 4 also shows that during milling, the severe plastic deformation and fracturing of particles were caused particle size of the sample reduced as shown in Figure 6. Figure 6 shows SEM image of sample milled for 50 hours.



(a) before milling



(b) after milling for 50 hours

Fig. 6 Surface morphology with SEM and TEM of α -Fe/C composite powders

From parameter lattice data shows that the particle size of graphite powders were reduced by fracturing along the basal plane and subsequent fracturing of the hexagonal network with milling process. In addition the particle size was decreased, is also suspected to have grown embryo of carbon nanotube due to the presence of iron due to iron is the most suitable pure-metal catalyst for the growth of aligned multiwall nanotubes [12]. Crystallization of the amorphous carbon takes place during the heat of high impact energy. Base on the TEM image, carbon (C_2H) is suspected to have been forming different morphologies after milled 50 h, such as nanotubes formation, possibly depending on nature of the nucleation regions.

Although nanotube has not been formed during the ball milling process, the heat of high impact energy is an essential step to form the nanotubes. Direct heating of the graphite powders without milling treatment does not cause any nanotube structures because graphite is very stable. The role of ball milling treatment is to create precursor containing nucleation structures and free carbons atoms [12-13]. In addition, the size of the carbon particles is one of the important factors for the formation of the nuclei of carbon nanotube. Carbon nanotubes grown from iron are

covered with amorphous carbon and carbon nanoparticles. The M-H hysteresis curve of the α -Fe/C composite samples before and after milling is shown in Figure 7.

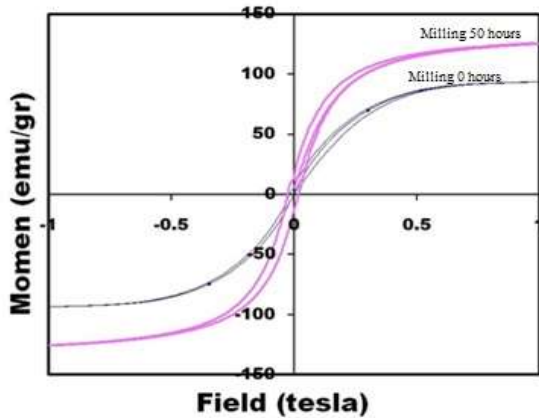


Fig.7 M-H hysteresis curves of α -Fe/C

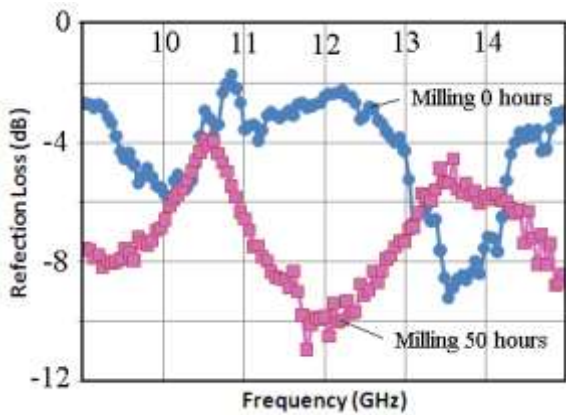


Fig.8 Reflection loss curves of α -Fe/C

The results of M-H hysteresis curve is given the value of the magnetic parameters M_s (Magnetization saturated), M_r (Magnetization remanence) and H_c (coercive field). M_s values obtained from the maximum value of the magnetic field can be generated by the material (peak value of hysteresis curve), M_r is the value of the magnetic field at the moment when the polarization equal to zero, and H_c obtained from polarization moment when the magnetic field equal to zero. In Table 2 is shown that the parameter values for the magnetic nanocomposite α -Fe/C after milling is greater than the α -Fe/C before milling.

Table 2 Magnetic properties of α -Fe/C nanocomposite

Milling time	Magnetic parameter values		
	M_s (emu/g)	M_r (emu/g)	H_c (Tesla)
0 hour	93.6	5.84	0.011
50 hours	125.4	13.73	0.028

This is the impact of the milling process and the increased strain caused internal change that can lead to changes in magnetic properties of a material. In other words that the milling factor can caused crystal deformation, namely

crystallographic defect on the sample. The existence of crystallographic defect affect the material properties. Defects can occur in the form of atomic vacancies. A defect can cause single monoatomic vacancies that induce magnetic properties. In addition, the particle size is smaller thereby affecting the magnetic interaction between Fe atoms, causing the value of M_s (saturated magnetization) increase. In this nanocomposite, carbon serves as a separator and useful for dispersing the magnetic particles become better through mechanical milling process to suppress Eddy current losses. Because the amount of carbon added to this composite relatively large, so that the Fe magnetic particles can be separated from each other by these carbon particles. While nanocomposite is still able to maintain its volume fraction with high magnetic properties, resulting in large permeability value. In addition, that the phase transformation of graphite caused mechanism of interaction between the spin magnetic moments of the Fe atoms in the crystal is changed too.

In Figure 8 is shown that there is absorption of electromagnetic waves in the frequency range of 9-15 GHz. It is shown that the maximum reflection loss reaches -10 dB at 12 GHz and the absorption range under -4 dB is from 11.2 to 15.5 GHz with 2 mm thickness. Properties of electromagnetic wave absorption is affected by magnetic loss. The contributors to magnetic loss, such as magnetic hysteresis, domain-wall displacement, and Eddy current loss. The hysteresis loss is mainly caused by the time lags of the magnetization vector behind the external electromagnetic-field vector. The domain wall displacement loss only occurs in multidomain magnetic materials rather than single domain structure. The α -Fe/C composites have high electric resistivity and the graphite shells of nanoparticle can have the effect of reducing the Eddy current loss. The Eddy current loss is related to the diameter of nanoparticles and the electric conductivity. Therefore, it can be explained that the magnetic loss in α -Fe/C nanocomposite is mainly caused by the natural resonance, to the exclusion of the magnetic hysteresis, domain-wall displacement, and Eddy current loss. Accordance to concept, the excellent electromagnetic wave absorptions result from the efficient complementarity between the relative permittivity and permeability in materials. If that act only loss magnetic or dielectric loss alone will result in the absorption of electromagnetic waves become weak due to the imbalance of the electromagnetic wave resonance.

4. CONCLUSION

Nanocomposite of α -Fe/C has showed good properties as electromagnetic wave absorber. It is related to the homogeneously dispersing nanoparticles in matrix, reducing the magnetic coupling effect between nanoparticles, increasing effective surface anisotropy of nanoparticles, and constructing the electromagnetic match in nanoscale geometry. The analysis with experimental data

shows that the maximum reflection loss reaches -10 dB at 12 GHz and the absorption range under -4 dB is from 11.2 to 15.5 GHz with 2 mm thickness. The α -Fe/C nanocomposite is obtained candidate materials have potential applications in the fields of microwave absorbing materials.

REFERENCES

- [1] P.H. Zhou, J.L. Xie, Y.Q. Liu, L.J. Deng, Composition dependence of microstructure, magnetic and microwave, properties in ball-milled FeSiB nanocrystalline flakes, *Journal of Magnetism and Magnetic Materials*, 320 (2008) 3390–3393.
- [2] Xian Wang, Rongzhou Gong, Hao Luo, Zekun Feng, Microwave properties of surface modified Fe–Co–Zr alloy flakes with mechanochemically synthesized polystyrene, *Journal of Alloys and Compounds* 480 (2009) 761–764.
- [3] Y Tang, Y Shao, K F Yao and Y X Zhong, Fabrication and microwave absorption properties of carboncoated cementite nanocapsules, *Nanotechnology*, 25 (2014) 035704 (5pp)
- [4] X. F. Zhang, X. L. Dong, a H. Huang, Y. Y. Liu, W. N. Wang, X. G. Zhu, B. Lv, and J. P. Lei, C. G. Lee, Microwave absorption properties of the carbon-coated nickel nanocapsules, *Appl. Phys. Lett.* 89, 053115, (2006).
- [5] S. Sugimoto et al., “GHz microwave absorption of a fine α -Fe structure produced by the disproportionation of $\text{Sm}_2\text{Fe}_{17}$ in hydrogen,” *J. Alloys Compounds* 330, 2002, pp. 301-306.
- [6] Jiu Rong Liu, Masahiro Itoh, and Ken-ichi Machida, Electromagnetic wave absorption properties of α -Fe/Fe₃B/Y₂O₃ nanocomposites in gigahertz range, *Appl. Phys. Lett.*, Vol. 83, No. 19, 10 November 2003, 4017-4019.
- [7] Hong Zhu, Haiyan Lin, Hongfan Guo, Liufang Yu, Microwave absorbing property of Fe-filled carbon nanotubes synthesized by a practical route, *Materials Science and Engineering B* 138 (2007) 101–104.
- [8] J. Fayos, "Possible 3D carbon structures as progressive intermediates in graphite to diamond phase transition Note: mathematical model", *Journal of Solid State Chemistry* 148, 278-285 (1999).
- [9] H. Lipson, A. R. Stokes, "The Structure of graphite", *Proceedings of the Royal Society of London, Series A: Mathematical and Physical Sciences* (76,1906-) 181, 101-105 (1942)
- [10] H.Fjellvag, B. C. Hauback, T. Vogt, S. Stolen, "Monoclinic nearly stoichiometric wustite at low temperatures Sample: Kjeller, T = 8 K", *American Mineralogist* 87, 347-349 (2002)
- [11] B.H. Toby, EXPGUI, a graphical user interface for GSAS, *J. Applied Crystallography*(2000).
- [12] Ömer Guler, Ertan Evin, Carbon nanotubes formation by short-time ball milling and annealing of graphite, *Optoelectronics and Advanced Materials – Rapid Communications* Vol. 6, No. 1-2, January-February 2012, p. 183 – 187.
- [13] Z.P. Huang, D.Z. Wang, J.G. Wen, M. Sennett, H. Gibson, Z.F. Ren, *Appl. Phys. A* 74, 387–391 (2002)

ACKNOWLEDGEMENTS

The authors gratefully acknowledge for the financial support and the research facilities provided by the Centre for Science and Technology of Advanced Materials, National Nuclear Energy Agency